Contextual Direct Position Determination for Path Loss Informed Localization

Licheng Zhao, Wenqiang Pu, Rui Zhou, Ming-Yi You, and Qingjiang Shi, *Member, IEEE*

***Abstract*—In this letter, we look into the emitter localization task within the Direct Position Determination (DPD) paradigm. This paradigm is by essence a largest eigenvalue problem which treats the channel attenuation variables as free parameters. We consider the channel fading physical rule on electromagnetic signal propagation and reformulate the traditional DPD problem with a channel contextual prior. Thereafter, we develop iterative optimization algorithms based on the majorization-minimization (MM) framework. Numerical results show that the proposed algorithms outperform the traditional DPD estimators with better localization performance.**

***Index Terms*—Emitter localization, direct position determination, channel contextual prior, majorization-minimization.**

I. Introduction

EMITTER localization holds significant importance in various application fields, particularly in signal processing, wireless communications, environmental monitoring, and geographical navigation [1]. Traditional localization methods mostly adopt a two-step scheme: the first step is parameter estimation, such as angle of arrival, time of arrival, and Doppler frequency shift estimation, and the second step is location inference with the aid of the estimated parameters and receiver coordinates. However, the classical methods are often suboptimal because they miss out the fundamental connection that all location-related parameters should imply the same location of the emission source. To take account of this inherent connection, Weiss developed the Direct Position Determination (DPD) paradigm for both single-emitter [1] and multiple-emitter [2] scenarios. In this letter, we choose to focus on the single-emitter situation.

Received 5 February 2025; revised 4 March 2025; accepted 5 March 2025. Date of publication 10 March 2025; date of current version 24 March 2025. The work of Licheng Zhao was supported in part by the National Nature Science Foundation of China under Grant 62206182 and in part by Guangdong Basic and Applied Basic Research Foundation under Grant 2024A1515010154. The work of Wenqiang Pu was supported by the National Nature Science Foundation of China under Grant 62101350. The work of Rui Zhou was supported in part by the National Nature Science Foundation of China under Grant 62201362 and in part by the Shenzhen Science and Technology Program under Grant RCBS20221008093126071. The associate editor coordinating the review of this article and approving it for publication was Prof. Giuseppe Thadeu Freitas de Abreu. *(Corresponding author: Wenqiang Pu.)*

Licheng Zhao, Wenqiang Pu, and Rui Zhou are with Shenzhen Research Institute of Big Data, Shenzhen 518172, China (e-mail: zhaolicheng@sribd.cn; wpu@sribd.cn; rui.zhou@sribd.cn).

Ming-Yi You is with the National Key Laboratory of Electromagnetic Space Security, Jiaxing 314033, China (e-mail: youmingyi@126.com).

Qingjiang Shi is with the School of Software Engineering, Tongji University, Shanghai 201804, China, and also with Shenzhen Research Institute of Big Data, Shenzhen 518172, China (e-mail: shiqj@tongji.edu.cn).

Digital Object Identifier 10.1109/LSP.2025.3550047

Consider a stationary emitter and M scattered receivers in the far field region. Each receiver contains a uniform linear array (ULA) with N antennas. The emitter location is *unknown* and to be estimated from the received signal samples. The transmitted signal at time slot t is represented as $s(t) \in \mathbb{C}$ and the m-th receiver captures a signal $\mathbf{x}_m(t) \in \mathbb{C}^M$ expressed as

$$\mathbf{x}_m(t) = \mathbf{a}_m(\mathbf{p})\, h_m s(t - \tau_m(\mathbf{p})) + \mathbf{n}_m(t), \tag{1}$$

where $\mathbf{p} \in \mathbb{R}^2$ is the planar coordinates of the emitter location, $\mathbf{a}_m(\mathbf{p}) \in \mathbb{C}^N$ is the array response of receiver m from location $\mathbf{p}$, $\tau_m(\mathbf{p}) = \mathrm{dist}_m(\mathbf{p})/c$ is the propagation time from location $\mathbf{p}$ to receiver m, $\mathrm{dist}_m(\mathbf{p})$ denotes the distance between receiver m and location $\mathbf{p}$, c stands for the speed of light, $h_m \in \mathbb{C}$ is a free parameter measuring channel path loss, and $\mathbf{n}_m(t)$ represents zero-mean complex white Gaussian noise. Every K signal samples are grouped into a section and rowwise Discrete Fourier Transform (DFT) is applied within each section. For any section index $j = 1, 2, \ldots$ and any $k = 0, \ldots, K-1$, the DFT transformed signal of the m-th receiver, $\bar{\mathbf{x}}_m(k,j)$, is expressed as

$$\begin{aligned}\bar{\mathbf{x}}_m(k,j) &= \mathbf{a}_m(\mathbf{p})\, h_m \bar{s}(k,j)\\ &\quad \cdot \exp\left(-j2\pi \frac{k}{K} f_s \tau_m(\mathbf{p})\right) + \bar{\mathbf{n}}_m(k,j),\end{aligned} \tag{2}$$

where $\bar{s}(k,j)$ is the DFT representation of $s(t)$ and f_s is the sampling rate. By vertically stacking the transformed signals of M receivers, i.e., $\bar{\mathbf{x}}(k,j) = [\bar{\mathbf{x}}_1(k,j); \ldots; \bar{\mathbf{x}}_M(k,j)]$ and $\bar{\mathbf{n}}(k,j) = [\bar{\mathbf{n}}_1(k,j); \ldots; \bar{\mathbf{n}}_M(k,j)]$, we obtain a compact signal representation:

$$\bar{\mathbf{x}}(k,j) = \mathbf{A}(k,\mathbf{p})\, \mathbf{h}\bar{s}(k,j) + \bar{\mathbf{n}}(k,j), \tag{3}$$

where $\mathbf{h} = [h_1, \ldots, h_M]^T \in \mathbb{C}^M$ is the channel attenuation vector, $\mathbf{A}(k,\mathbf{p}) = \mathrm{Blkdiag}\{\mathbf{b}_1(\mathbf{p}), \ldots, \mathbf{b}_M(\mathbf{p})\}$ which constructs a block diagonal matrix as $\begin{bmatrix}\mathbf{b}_1(\mathbf{p}) & & \\ & \ddots & \\ & & \mathbf{b}_M(\mathbf{p})\end{bmatrix}$, and $\mathbf{b}_m(\mathbf{p}) = \mathbf{a}_m(\mathbf{p}) \exp(-j2\pi \frac{k}{K} f_s \tau_m(\mathbf{p}))$, $\forall m$. The DPD paradigm [1], [2], [3] constructs a statistic of $\mathbf{M}(\mathbf{p})$ in the following form:

$$\mathbf{M}(\mathbf{p}) = \sum_{k=0}^{K-1} \mathbf{A}^H(k,\mathbf{p})\, \rho(\mathbf{R}_k) \mathbf{A}(k,\mathbf{p}), \tag{4}$$

where $\mathbf{R}_k = \frac{1}{J}\sum_{j=1}^{J} \bar{\mathbf{x}}(k,j)\bar{\mathbf{x}}^H(k,j)$ and $\rho(\mathbf{R}) : \mathbb{H}^M \mapsto \mathbb{H}^M$ is a multivariate function on covariance matrix $\mathbf{R}$. As a result, the DPD problem is formulated as a largest eigenvalue problem, written as:

$$\underset{\mathbf{h}:\|\mathbf{h}\|_2=1}{\text{maximize}} \quad \mathbf{h}^H \mathbf{M}(\mathbf{p})\, \mathbf{h}. \tag{5}$$

When the ML estimator is adopted [3], $\rho(\mathbf{R}) = \mathbf{R}$; when the MVDR rationale is applied [3], $\rho(\mathbf{R}) = \mathbf{R}^{-1}$ and problem (5) is converted to minimization; when the principles of MUSIC algorithm are followed [2], $\rho(\mathbf{R}) = \mathbf{U}\mathbf{U}^H$ where $\mathbf{U}$ is composed of the eigenvectors corresponding to the k-largest eigenvalues. The optimal value of problem (5) is the largest eigenvalue of $\mathbf{M}(\mathbf{p})$, written as $\lambda_{\max}(\mathbf{M}(\mathbf{p}))$. Subsequently, the emitter location can be obtained from a grid search over a predefined bounded region $\mathcal{P}$ that maximizes the largest eigenvalues, i.e.,

$$\mathbf{p}^\star = \arg\max_{\mathbf{p}\in\mathcal{P}} \lambda_{\max}(\mathbf{M}(\mathbf{p})). \tag{6}$$

The current DPD paradigm treats the channel attenuation vector $\mathbf{h}$ as free parameters independent of the emitter location, neglecting the channel fading effect in the process of electromagnetic signal propagation. Actually, the magnitude of each channel coefficient should be inversely proportional to the $\gamma/2$-th power of the propagation distance and and scaled by a log-normal shadowing factor ξ [4, Chap. 2]. Thus, the consideration of the channel fading rule in DPD paradigm improves modeling accuracy, but the proper way of mathematical implementation remains unclear.

Our work is based on the hypothesis that using *channel contextual prior* (like path loss) in the traditional DPD method would produce better localization results. This prior can be naturally embedded into problem (5), giving rise to a *context-constrained* DPD problem:

$$\underset{\mathbf{h}:\|\mathbf{h}\|_2=1,\ \underbrace{\mathbf{h}\in\mathcal{H}(\mathbf{p})}_{\text{contextual prior}}}{\text{maximize}} \quad \mathbf{h}^H \mathbf{M}(\mathbf{p})\mathbf{h}, \tag{7}$$

where $\mathcal{H}(\mathbf{p}) \subseteq \mathbb{C}^M$ is a location-aware contextual feasible set and $\mathbf{p}$ serves as the context for channel prior. This problem is named as the contextual DPD problem. The contribution of this work is two-fold: 1) we incorporate the channel contextual prior in the DPD problem, as opposed to the traditional formulation which treats path loss as free parameters, and 2) while the traditional DPD method solves a largest-eigenvalue problem, we develop iterative optimization algorithms using the majorization-minimization (MM) framework [5], introducing a new style of solution.

II. Problem Formulation

For modeling improvement, we exploit the physical rule on electromagnetic signal propagation and establish a connection between $\mathbf{p}$ and h_m by introducing a path loss prior. To be specific, the channel coefficient h_m is modeled as a location-dependent path loss $h_m(\mathbf{p})$ and

$$|h_m(\mathbf{p})| \propto \frac{\xi_m}{[\text{dist}_m(\mathbf{p})]^{\gamma/2}}, \tag{8}$$

with ξ_m's being independent and identically distributed (i.i.d) log-normal random variables of mean μ and variance σ^2.

In order to incorporate the path loss (8) into a contextual constraint set $\mathcal{H}(\mathbf{p})$, we perform pairwise division between $|h_m|$ and $|h_1|$ for any $m > 1$:

$$\frac{|h_m|}{|h_1|} = \frac{\xi_m}{\xi_1}\left[\frac{\text{dist}_1(\mathbf{p})}{\text{dist}_m(\mathbf{p})}\right]^{\gamma/2} = \frac{\xi_m}{\xi_1} d_{1,m}^{\gamma/2}(\mathbf{p}), \tag{9}$$

where $d_{1,m}(\mathbf{p}) = \text{dist}_1(\mathbf{p})/\text{dist}_m(\mathbf{p})$. Since ξ_m's are i.i.d log-normal random variables, $\log(\xi_m/\xi_1)$'s are identically Gaussian distributed with zero mean and variance $2\sigma^2$. According to the concentration property of Gaussian distribution, for any $m > 1$, there always exists a finite-length interval $[-U_m, U_m]$ ($U_m > 0$) such that the event

$$-U_m \le \log\left(\frac{|h_m|}{|h_1|} d_{1,m}^{-\gamma/2}(\mathbf{p})\right) \le U_m \tag{10}$$

occurs with a given probability $P < 1$. In this case, $U_m = \sqrt{2}\sigma\Phi^{-1}(\frac{1+P}{2})$ and Φ is the cumulative distribution function of the standard Gaussian distribution. Note that $\log(\xi_m/\xi_1)$'s are identically distributed, and therefore the value of U_m is index invariant for a given P. Setting P close enough to 1, we deduce that the path loss knowledge can be transformed with high probability into a contextual constraint set, given as

$$\mathcal{H}(\mathbf{p}) = \left\{\mathbf{h} \middle| d_{1,m}^{\gamma/2}(\mathbf{p}) \cdot l \le \frac{|h_m|}{|h_1|} \le d_{1,m}^{\gamma/2}(\mathbf{p}) \cdot u, \forall m > 1\right\}, \tag{11}$$

where $u = \exp(\sqrt{2}\sigma\Phi^{-1}(\frac{1+P}{2}))$ and $l = \exp(-\sqrt{2}\sigma\Phi^{-1}(\frac{1+P}{2}))$. In words, the path loss ratio $\frac{|h_m|}{|h_1|}$ is constrained within an interval that depends on $\mathbf{p}$ and receiver positions. In practical implementation, l and u are customized hyperparameters. In this letter, we adopt the MVDR estimator, i.e., $\mathbf{M}(\mathbf{p}) = \sum_{k=0}^{K-1} \mathbf{A}^H(k,\mathbf{p})\mathbf{R}_k^{-1}\mathbf{A}(k,\mathbf{p})$, and solve a minimization problem. Eventually, the contextual DPD problem is described as

$$\underset{\mathbf{h}}{\text{minimize}} \quad \mathbf{h}^H\mathbf{M}\mathbf{h} \tag{12a}$$

$$\text{subject to} \quad d_{1,m}^{\gamma/2} \cdot l \le \frac{|h_m|}{|h_1|} \le d_{1,m}^{\gamma/2} \cdot u, \forall m > 1, \tag{12b}$$

$$\|\mathbf{h}\|_2 = 1, \tag{12c}$$

where $d_{1,m}$ is an abbreviation for $d_{1,m}(\mathbf{p})$. The emitter location is selected as the grid point in $\mathcal{P}$ achieving the maximum of objective reciprocals of (12) [3].

III. Contextual DPD Optimization

In this section, we present an algorithmic solution to the contextual DPD problem. We are going to apply the MM framework in pursuit of an iterative algorithm with stationarity convergence guarantees. The solution to problem (12) will be discussed in two separate scenarios, as are elaborated below.

A. Exact Path Loss Exponent

When the path loss exponent γ is exactly known, $\mathbf{h}$ is the only optimization variable. In the free space environment, γ is equal to 2 [6] and we take this environmental condition as an illustrative example. The first step of the MM framework is to construct a majorizing function. The q-th iterate of $\mathbf{h}$ is represented as $\mathbf{h}^{(q)}$. In order to elementwisely decouple the variable $\mathbf{h}$, we majorize the quadratic objective at $\mathbf{h}^{(q)}$ by [7, Lemma 1]:

$$\mathbf{h}^H\mathbf{M}\mathbf{h} \leq \left(\mathbf{h}^{(q)}\right)^H \left(\|\mathbf{M}\|_2 \mathbf{I} - \mathbf{M}\right)\mathbf{h}^{(q)} + 2\mathrm{Re}\left[\mathbf{h}^H\mathbf{b}\right] + \|\mathbf{M}\|_2 \cdot \mathbf{h}^H\mathbf{h}, \tag{13}$$

where $\mathbf{b} = (\mathbf{M} - \|\mathbf{M}\|_2\mathbf{I})\mathbf{h}^{(q)}$. The second step is to solve the minimization problem. The first term of (13) is a constant. Besides, the last term is also a constant due to the constraint $\|\mathbf{h}\|_2 = 1$. Removing all the constant terms, we obtain the following minimization problem:

$$\underset{\mathbf{h}}{\text{minimize}} \quad 2\mathrm{Re}\left[\mathbf{h}^H\mathbf{b}\right] \tag{14a}$$

$$\text{subject to} \quad d_{1,m}l \leq \frac{|h_m|}{|h_1|} \leq d_{1,m}u, \forall m > 1, \tag{14b}$$

$$\|\mathbf{h}\|_2 = 1. \tag{14c}$$

We notice that the phase of $\mathbf{h}$ does not affect the feasibility in problem (14), so the optimal phase solution of $\mathbf{h}$ is only related to $\mathbf{b}$ and

$$\arg\left(\mathbf{h}^\star\right) = \arg\left(\mathbf{b}\right) + \pi. \tag{15}$$

Thus, we can concentrate on magnitude optimization. We denote $|\mathbf{h}|$ and $|\mathbf{b}|$ as $\tilde{\mathbf{h}}$ and $\tilde{\mathbf{b}}$, respectively, and problem (14) becomes

$$\underset{\tilde{\mathbf{h}}}{\text{minimize}} \quad -2\tilde{\mathbf{h}}^T\tilde{\mathbf{b}} \tag{16a}$$

$$\text{subject to} \quad d_{1,m}l \cdot \tilde{h}_1 \leq \tilde{h}_m \leq d_{1,m}u \cdot \tilde{h}_1, \forall m > 1, \tag{16b}$$

$$\tilde{\mathbf{h}}^T\tilde{\mathbf{h}} = 1. \tag{16c}$$

The first constraint of (16) is linear while the second one is still nonconvex, so we do a change of variable $\tilde{\mathbf{g}} = \tilde{\mathbf{h}} \odot \tilde{\mathbf{h}}$ ($\odot$ is the Hadamard product) and derive the following equivalent convex reformulation:

$$\underset{\tilde{\mathbf{g}}}{\text{minimize}} \quad -2\sum_{m=1}^{M} \tilde{b}_m \sqrt{\tilde{g}_m} \tag{17a}$$

$$\text{subject to} \quad \left(d_{1,m}l\right)^2 \cdot \tilde{g}_1 \leq \tilde{g}_m \leq \left(d_{1,m}u\right)^2 \cdot \tilde{g}_1, \forall m > 1, \tag{17b}$$

$$\mathbf{1}^T\tilde{\mathbf{g}} = 1. \tag{17c}$$

We successively solve problem (17) via an off-the-shelf solver until convergence.

B. Inexact Path Loss Exponent

When the path loss exponent γ is not exactly known but lies within an interval $[\gamma_l, \gamma_u]$, we can still apply the MM framework. The majorization step and the optimal phase solution follow the previous case but the minimization problem on magnitude is slightly different:

$$\underset{\tilde{\mathbf{h}},\gamma}{\text{minimize}} \quad -2\tilde{\mathbf{h}}^T\tilde{\mathbf{b}} \tag{18a}$$

$$\text{subject to} \quad d_{1,m}^{\gamma/2}l \leq \frac{\tilde{h}_m}{\tilde{h}_1} \leq d_{1,m}^{\gamma/2}u, \forall m > 1, \tag{18b}$$

$$\gamma_l \leq \gamma \leq \gamma_u, \tag{18c}$$

$$\tilde{\mathbf{h}}^T\tilde{\mathbf{h}} = 1. \tag{18d}$$

To solve problem (18), we relax the equality constraint $\tilde{\mathbf{h}}^T\tilde{\mathbf{h}} = 1$ to be inequality and the relaxation is tight without affecting optimality. The reason is given by contradiction. Suppose that the norm of optimal $\tilde{\mathbf{h}}$ is strictly less than 1, i.e., $\|\tilde{\mathbf{h}}^\star\|_2 < 1$, and we can always scale up $\tilde{\mathbf{h}}^\star$ by $1/\|\tilde{\mathbf{h}}^\star\|_2 (> 1)$ without violating the constraints. However, the objective function value decreases: $-1/\|\tilde{\mathbf{h}}^\star\|_2 \cdot (\tilde{\mathbf{h}}^\star)^T\tilde{\mathbf{b}} < -(\tilde{\mathbf{h}}^\star)^T\tilde{\mathbf{b}}$, which contradicts the optimality assumption. After relaxation, we do a change of variable: $\tilde{h}_m = \exp(\tilde{g}_m)$, and problem (18) is recast as

$$\underset{\tilde{\mathbf{g}},\gamma}{\text{minimize}} \quad -2\sum_{m=1}^{M} \tilde{b}_m \exp\left(\tilde{g}_m\right) \tag{19a}$$

$$\text{subject to} \quad \tfrac{\gamma}{2}\log d_{1,m} + \log l \leq \tilde{g}_m - \tilde{g}_1 \leq \tfrac{\gamma}{2}\log d_{1,m} + \log u, \forall m > 1, \tag{19b}$$

$$\gamma_l \leq \gamma \leq \gamma_u, \tag{19c}$$

$$\log\left[\sum_{m=1}^{M} \exp\left(2\tilde{g}_m\right)\right] \leq 0. \tag{19d}$$

The last constraint is expressed in a "log-sum-exp" format for numerical stability.

To this point, the constraint set is convex but the objective is not. We consider solving (19) with an inner loop using MM as well. In view of the concavity of $-\exp(x)$, we further majorize the objective with its first order Taylor expansion at the current iterate $\tilde{g}_m^{(q)}$:

$$-2\sum_{m=1}^{M} \tilde{b}_m \exp\left(\tilde{g}_m\right) \leq -2\sum_{m=1}^{M} \tilde{b}_m \exp\left(\tilde{g}_m^{(q)}\right) - 2\sum_{m=1}^{M} \tilde{b}_m \cdot \exp\left(\tilde{g}_m^{(q)}\right)\left(\tilde{g}_m - \tilde{g}_m^{(q)}\right). \tag{20}$$

Removing all the constant terms, we obtain the inner minimization problem:

$$\underset{\tilde{\mathbf{g}},\gamma}{\text{minimize}} \quad -2\sum_{m=1}^{M} \tilde{b}_m \exp\left(\tilde{g}_m^{(q)}\right)\tilde{g}_m \tag{21a}$$

$$\text{subject to} \quad \tfrac{\gamma}{2}\log d_{1,m} + \log l \leq \tilde{g}_m - \tilde{g}_1 \leq \tfrac{\gamma}{2}\log d_{1,m} + \log u, \forall m > 1, \tag{21b}$$

$$\gamma_l \leq \gamma \leq \gamma_u, \tag{21c}$$

$$\log\left[\sum_{m=1}^{M} \exp\left(2\tilde{g}_m\right)\right] \leq 0. \tag{21d}$$

The overall solution scheme is a double loop and problem (21) is iteratively solved until convergence.

IV. Simulation

In this section, we present simulation results to evaluate the performance of the proposed algorithm. All simulations are performed on a PC with a 2.90 GHz i7-10700 CPU and 16.0 GB RAM. The benchmark algorithm is DPD-HR in [3]. The proposed algorithm is based on the MVDR estimator and additionally considers channel contextual prior. For simplicity, the proposed algorithms are named as Contextual-Exact (Section III-A) and Contextual-Inexact (Section III-B).

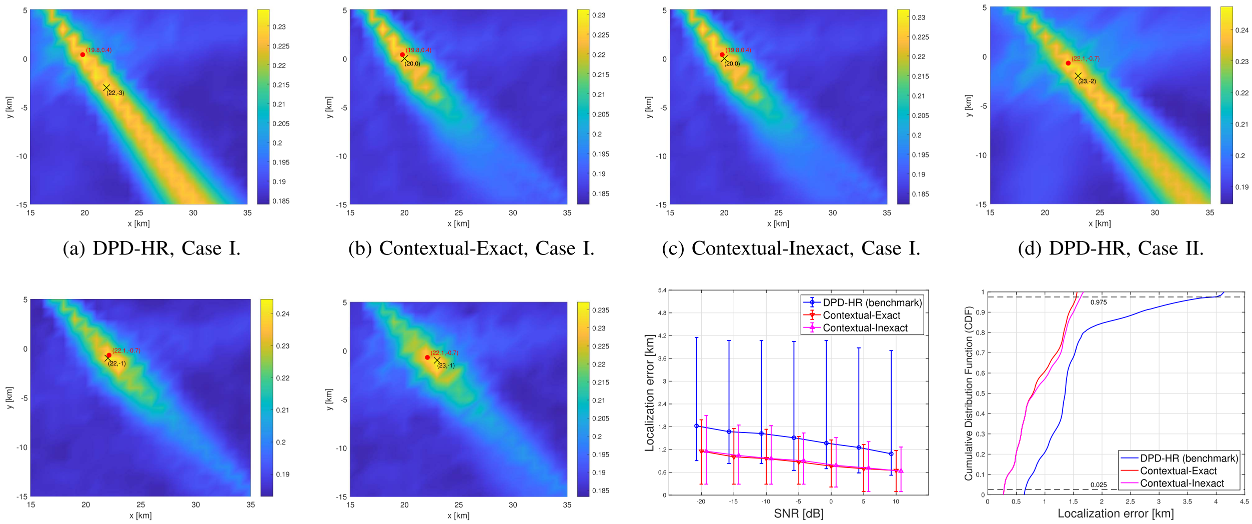

(a) DPD-HR, Case I. (b) Contextual-Exact, Case I. (c) Contextual-Inexact, Case I. (d) DPD-HR, Case II.

(e) Contextual-Exact, Case II. (f) Contextual-Inexact, Case II. (g) Average localization error. (h) CDF of localization error.

Fig. 1. Miscellaneous numerical results.

We focus on the single emitter scenario and consider two distinct emitter location cases. In Case I, the emitter's location is $(19.8, 0.4)$ km and in Case II, the location is $(22.1, -0.7)$ km. In both cases, the emitter transmits narrowband quaternary phase shift keying (QPSK) signals. Five receivers ($M = 5$) are placed in the far field region of the emitter at coordinates $(-21, -12)$, $(12, 12)$, $(40, -20)$, $(55, 7)$, and $(10, -52)$ km, each equipped with 10 antennas ($N = 10$) at half-wavelength spacing. The magnitude of channel coefficient is characterized by (8) with ξ_m's being i.i.d and $\log \xi_m \sim \mathcal{N}(0, 0.003)$. The phase is uniformly distributed between 0 and 2π. Sampling frequency f_s is 120 kHz, observation time T is 0.5 seconds, DFT sequence length K is 512, and thus the total number of sections J is floor$((f_sT)/K) = 117$. The search region for emitter localization is specified as a square area and the coordinates of the four corners are $(15, -15)$, $(35, -15)$, $(15, 5)$, and $(35, 5)$ km. This area is evenly divided into 20×20 grids and the evaluation is conducted on the grid point (edges included). When γ is not exactly known, we assume $\gamma \in [1.8, 2.2]$ by default. Each antenna array is oriented to the geometric center of the search region and the reference receiver is selected as the closest node to the center.

Case I: As shown in Fig. 1(a), (b), and (c), the proposed algorithms can spot the target with greater precision than the benchmark at a -5 dB received SNR on the reference node. The black cross is the estimated position and the red dot is the ground truth. The benchmark DPD-HR causes a localization error of 4.05 km while the error distance of the proposed algorithms is merely 0.45 km. *Case II:* when the emitter is shifted to $(22.1, -0.7)$ km, the proposed algorithms occasionally give different localization results at a 0 dB received SNR, cf. Fig. 1(d), (e), and (f). The localization error of DPD-HR is 1.58 km while those of Contextual-Exact and Contextual-Inexact are 0.32 km and 0.95 km, respectively.

Next, we extend the SNR range for further algorithmic examination. The simulation results are presented in Fig. 1(g) and (h). The received SNR on the reference node varies from -20 dB to 10 dB. The emitter location is uniformly randomized within the detection region. In Fig. 1(g), each reported data point is averaged over 150 random instances. In terms of average performance, both proposed algorithms always reach a lower localization error level than the benchmark. Quantitatively, the average improvement to DPD-HR is about 40% for both Contextual-Exact and Contextual-Inexact. However, of all the compared algorithms, the estimates demonstrate high volatility, so we plot a 95% confidence interval around the mean value (cf. Fig. 1(g)) and also investigate the cumulative distribution function (CDF) of the estimates at a -5 dB received SNR (cf. Fig. 1(h)). From Fig. 1(g), we can deduce that the proposed algorithms offer better guarantees against extreme error levels because the upper limits of confidence intervals generated by the proposed algorithms are about 60% lower than the benchmark. In Fig. 1(h), we increase the number of random instances to 400 and observe that in Case I, the error level of DPD-HR is quite extreme and very close to the boundary of the confidence interval while those of Contextual-Exact and Contextual-Inexact are controllable.

V. Conclusion

In this letter, we have investigated into emitter localization within the DPD paradigm for end-to-end optimization. In the traditional DPD paradigm, the channel attenuation vector is independent of the emitter location. By contrast, we have considered the channel fading effect on signal propagation and improved the system modeling with a contextual prior. The essence of the contextual DPD problem is to incorporate prior information as optimization constraints. To solve the contextual DPD problem, we have put forward iterative optimization algorithms using the MM framework. We have derived a convex formulation for variable update in every iteration. Numerical results have revealed that the proposed algorithms are superior to the traditional DPD estimators. An interesting finding is that the concept of contextual optimization can be extended to other data processing fields such as data clustering tasks [8]. The class-dependent characteristics like clustering centre, scattering pattern, and/or statistical distribution could be modeled as contextual constraints, which may enhance the accuracy of the clustering results.

REFERENCES

[1] A. J. Weiss, "Direct position determination of narrowband radio frequency transmitters," *IEEE Signal Process. Lett.*, vol. 11, no. 5, pp. 513–516, May 2004.

[2] A. J. Weiss and A. Amar, "Direct position determination of multiple radio signals," *EURASIP J. Adv. Signal Process.*, vol. 2005, pp. 1–13, 2005.

[3] T. Tirer and A. J. Weiss, "High resolution direct position determination of radio frequency sources," *IEEE Signal Process. Lett.*, vol. 23, no. 2, pp. 192–196, Feb. 2016.

[4] A. Goldsmith, *Wireless Communications*. Cambridge, U.K.: Cambridge Univ. Press, 2005.

[5] Y. Sun, P. Babu, and D. P. Palomar, "Majorization-minimization algorithms in signal processing, communications, and machine learning," *IEEE Trans. Signal Process.*, vol. 65, no. 3, pp. 794–816, Feb. 2016.

[6] M. Viswanathan, *Wireless Communication Systems in Matlab*. India: Mathuranathan Viswanathan, 2020.

[7] J. Song, P. Babu, and D. P. Palomar, "Sequence design to minimize the weighted integrated and peak sidelobe levels," *IEEE Trans. Signal Process.*, vol. 64, no. 8, pp. 2051–2064, Apr. 2016.

[8] J. V. de Miranda Cardoso, J. Ying, and D. P. Palomar, "Learning bipartite graphs: Heavy tails and multiple components," *Adv. Neural Inf. Process. Syst.*, vol. 35, pp. 14044–14057, 2022.